

# A dynamical and kinematical model of the Galactic stellar halo and possible implications for galaxy formation scenarios

J. Sommer-Larsen<sup>1</sup>, T.C. Beers<sup>5</sup>, C. Flynn<sup>3,4</sup>,  
R. Wilhelm<sup>5</sup> and P. R. Christensen<sup>1,2</sup>

1) Theoretical Astrophysics Center  
Juliane Maries Vej 30, DK-2100 Copenhagen Ø, Denmark  
(jslarsen@tac.dk)

2) The Niels Bohr Institute  
Blegdamsvej 17, DK-2100 Copenhagen Ø, Denmark  
(perrex@nbi.dk)

3) NORDITA  
Blegdamsvej 17, DK-2100 Copenhagen Ø, Denmark

4) Tuorla Observatory  
Piikkiö, FIN-21500, Finland  
(cflynn@astro.utu.fi)

5) Department of Physics and Astronomy  
Michigan State University, E. Lansing Michigan 48824, USA  
(beers@pa.msu.edu, wilhelm@pa.msu.edu)

*Submitted to The Astrophysical Journal*

# Abstract

We re-analyse the kinematics and dynamics of the system of blue horizontal branch field (BHBF) stars in the Galactic halo (in particular the outer halo), fitting the kinematics with the model of radial and tangential velocity dispersions in the halo as a function of galactocentric distance  $r$  proposed by Sommer-Larsen, Flynn & Christensen (1994), but making use of a much larger sample of BHBF stars than was previously available. The present sample consists of nearly 700 Galactic halo BHBF stars.

A very good fit to the observations is obtained. The basic result is that the radial component,  $\sigma_r$ , of the stellar halo's velocity ellipsoid decreases fairly rapidly beyond the solar circle. The observed decrease is from  $\sigma_r \simeq 140 \pm 10 \text{ km s}^{-1}$  at the sun, to an asymptotic value of  $\sigma_r = 89 \pm 19 \text{ km s}^{-1}$  at large  $r$ . The rapid decrease in  $\sigma_r$  is matched by an increase in the tangential velocity dispersion,  $\sigma_t$ , with increasing  $r$ . Thus, the character of the stellar halo velocity ellipsoid is shown to change markedly from radial anisotropy at the sun to tangential anisotropy in the outer parts of the Galactic halo ( $r \gtrsim 20 \text{ kpc}$ ).

The implications of our results for possible Galactic formation scenarios are discussed. Our results may indicate that the Galaxy formed hierarchically (partly or fully) through merging of smaller subsystems - the 'bottom-up' galaxy formation scenario, which for quite a while has been favoured by most theorists and recently also has been given some observational credibility by HST observations of a potential group of small galaxies, at high redshift, possibly in the process of merging to a larger galaxy.

*Subject headings:* Galaxy: halo – kinematics and dynamics – formation – stars: horizontal-branch – kinematics

# 1 Introduction

Although the stellar halo accounts for only about 1% of the luminous mass of the Galaxy, it plays an crucial role in studies of the Galaxy’s formation, evolution, and present-day structure. The halo has long been considered the Galaxy’s oldest component, age estimates being tractable for its most conspicuous constituent, the metal-weak globular clusters, as well as for (with less certainty) individual metal-weak stars. Thus the dynamical and chemical state of the luminous halo population provides information on the formation of large disk galaxies such as the Milky Way. Furthermore, luminous halo-population objects can be treated as dynamical tracers in order to estimate the mass of the Galaxy’s dark-matter halo, which increasingly dominates the Galaxy’s mass at large galactocentric distances.

At present, the best measurements of the halo’s kinematics are obtained from analysis of the motions of stars found in the solar neighbourhood; traditionally from samples of high-proper-motion stars (Ryan & Norris 1991; Carney et al. 1994), more recently from kinematically-unbiased samples of metal-weak stars (see Beers & Sommer-Larsen 1995, and references therein). In order to obtain samples of halo-population stars *in situ*, methods have been developed to find distant weak-lined K giants (Ratnatunga & Freeman 1989; Morrison, Flynn, & Freeman 1990), RR Lyrae stars (e.g. Hawkins 1984) and blue horizontal-branch field (hereafter, BHBF) stars (Flynn, Sommer-Larsen & Christensen 1994, 1995, and references therein; Kinman, Suntzeff, & Kraft 1994; Wilhelm, Beers, & Gray 1997). Particular advantages of BHBF stars include the fact that they are much easier to confidently identify than metal-weak K giants and also considerably easier to identify than RR Lyrae stars. BHBF stars are also much more numerous than, for example, the RR Lyraes, and their line-of-sight velocities can be determined comparatively much easier and with higher accuracy.

In this paper we analyse the kinematics of a large sample of BHBF stars in the outer halo. We have supplemented the sample of 133 stars used in a recent analysis of the kinematics and dynamics of the system of BHBF stars of the outer Galactic halo by Sommer-Larsen, Flynn & Christensen (1994, hereafter SLFC94) with an additional 546 stars (for a total of 679 BHBF stars), the majority of which were originally identified in the HK survey of Beers and colleagues (Beers et al. 1996, and references therein), and analysed using techniques developed by Wilhelm (1995). The data are described in section 2. In section 3 we fit the simple model, proposed by SLFC94 for the dependence of the radial and tangential velocity dispersions of the halo as a function of galactocentric distance  $r$ , to the enlarged data sample. We find that the radial component of the velocity ellipsoid of the outer stellar halo is remarkably low, compared to the value at the sun of  $\sigma_{r,\odot} \simeq 140 \text{ km s}^{-1}$ , reaching an asymptotic value of  $\sigma_r \simeq 89 \text{ km s}^{-1}$  at large  $r$ , and that the velocity ellipsoid in the outer halo is tangentially anisotropic, in contrast to the local halo velocity ellipsoid, which is radially anisotropic. A discussion of the results obtained and their implications, in particular for galaxy

formation scenarios, is presented in section 4. Finally in section 5 we summarize our conclusions.

## 2 The data

The SLFC94 model is constrained by a specification of the halo velocity ellipsoid in the vicinity of the sun, and line-of-sight velocity measurements of halo BHBF stars in various fields over a range of galactocentric distances from approximately 7 kpc to 65 kpc.

In the solar neighborhood the components of the velocity ellipsoid in the halo are well known. Norris, Bessell & Pickles (1985) find  $\vec{\sigma} = (\sigma_r, \sigma_\phi, \sigma_\theta) = (125 \pm 11, 96 \pm 9, 88 \pm 7) \text{ km s}^{-1}$  for halo objects defined as  $[\text{Fe}/\text{H}] < -1.2$ . Morrison, Flynn & Freeman (1990) found that the kinematics of the halo and thick disk overlap in the range  $-1.6 < [\text{Fe}/\text{H}] < -1.0$ . In an attempt to isolate the 'true' halo, these authors used only stars with  $[\text{Fe}/\text{H}] < -1.6$  to derive  $\vec{\sigma} = (133 \pm 8, 98 \pm 13, 94 \pm 6) \text{ km s}^{-1}$ . Beers & Sommer-Larsen (1995) also found significant evidence for an extension of the thick disk well into the metallicity range usually identified with the Galactic halo. After correction for the effects of thick-disk stars in the solar neighbourhood, they derived a halo velocity ellipsoid of  $\vec{\sigma} = (153 \pm 10, 93 \pm 18, 107 \pm 7) \text{ km s}^{-1}$ . Considering the above, the radial velocity dispersion at the sun is about  $140 \text{ km s}^{-1}$  and the tangential components ( $\sigma_\phi$  and  $\sigma_\theta$ ) are about 90 - 100  $\text{km s}^{-1}$ . As is well known, the local halo velocity ellipsoid is consequently quite radially anisotropic.

SLFC94 analysed a sample of 133 outer halo BHBF stars mainly located in four fields: GP (NGP/SGP),  $(l, b) = (0^\circ, \pm 90^\circ)$ , F117,  $(l, b) = (270^\circ, -45^\circ)$ , SA287,  $(l, b) = (0^\circ, -47^\circ)$  and 22HR,  $(l, b) = (38^\circ, -51^\circ)$ . Over the past few years, we have obtained followup spectroscopy and broadband photometry for a sample of some 1000 field horizontal-branch and other A-type stars identified in the HK survey of Beers and collaborators. Wilhelm (1995), and Wilhelm, Beers, & Gray (1997) discuss techniques which are suitable for isolating a relatively pure sample of BHBF stars from this data set. A paper describing the full data set is presently in preparation (Wilhelm et al. 1997). For the purposes of the present analysis, we have combined available data from the the Wilhelm et al. catalog with previously-published BFHB stars (including stars identified as FHB from Norris 1986; Arnold & Gilmore 1992; Beers, Preston, & Shectman 1992; and Kinman, Sunzteff, & Kraft 1994), obtaining a total of 546 additional BHBF stars. The additional BHBF stars are located (within a radius of  $10^\circ$ ) in the GP fields, the SA287 field (plus one symmetric reflection - at  $(l, b) = (0^\circ, 47^\circ)$ , and the F117 and 22HR fields (plus three symmetric reflections - at  $(l, b) = (270^\circ, 45^\circ), (90^\circ, -45^\circ), (90^\circ, 45^\circ)$  and  $(38^\circ, 51^\circ), (322^\circ, -51^\circ), (322^\circ, 51^\circ)$ , respectively). The addition of stars in the 'reflection' fields obviously requires an assumption that the halo is axially symmetric and symmetric about the Galactic disk plane. We also assume that

the mean rotation of the halo is essentially zero (as found by, e.g., Sommer-Larsen & Christensen 1989 and Beers & Sommer-Larsen 1995). Mild violation of these assumptions will not have serious impact on our analysis but one should note that there are some indications of kinematic substructure in the halo (Majewski et al. 1996 and references therein).

In three of the four fields, including reflections, (GP, SA287 and 22HR), we have divided the stars into four bins, defined so that each bin covers a well-defined range in galactocentric radius  $r$ . In the field F117, including reflections, we have fewer stars than in the three other fields and have only used three bins. For each bin, we have calculated the line-of-sight velocity dispersion  $\sigma_{\text{los}}$ . The results are given in Table 1. The mean distance from the sun  $\langle d \rangle$ , the mean galactocentric distance  $\langle r \rangle$ , the mean value of the geometric projection factor  $\langle \gamma \rangle$  (equation 6 below) and the number of stars  $N$  in each bin are also listed.

Recalling that for larger  $r$ , the line-of-sight velocity dispersion  $\sigma_{\text{los}}$  is essentially a measure of  $\sigma_r$ , the clear implication of Table 1 is that the radial velocity dispersion of the outer halo is significantly lower than that found in the solar neighbourhood. In the most distant bin in F117,  $\sigma_{\text{los}} = 107 \pm 24 \text{ km s}^{-1}$  at  $r \simeq 21$  kpc, in 22<sup>h</sup>,  $\sigma_{\text{los}} = 112 \pm 12 \text{ km s}^{-1}$  at  $r \simeq 16$  kpc, in SA287,  $\sigma_{\text{los}} = 113 \pm 20 \text{ km s}^{-1}$  at  $r \simeq 13$  kpc, and at the GP,  $\sigma_{\text{los}} = 99 \pm 19 \text{ km s}^{-1}$  at  $r \simeq 19$  kpc. For the very distant stars ( $r \gtrsim 45$  kpc), the measured line-of-sight velocity dispersion is  $100 \pm 23 \text{ km s}^{-1}$  at a mean galactocentric distance of  $54 \pm 2$  kpc. In summary, the data suggest that  $\sigma_r$  decreases from about  $140 \text{ km s}^{-1}$  locally to about  $90$ – $110 \text{ km s}^{-1}$  at large  $r$ .

### 3 The model fit

The model is described in detail in SLFC94 and is briefly recapitulated here to make this paper more easily readable.

It is generally found that for  $r \gtrsim r_{\odot}$ , where  $r_{\odot} = 8.0$  kpc is the solar galactocentric distance, the stellar halo is approximately spherical - see, e.g., the review by Freeman (1987) and references therein; Hartwick (1987); Sommer-Larsen & Zhen (1990); Yamagata & Yoshii (1992), but note that there are indications that the inner halo is somewhat flattened (e.g. Hartwick 1987; Larsen & Humphries 1994; Wetterer & McGraw 1996). In this paper we shall be concerned with the properties of the outer Galactic halo and consequently the outer stellar halo (as traced by BHBF stars) is assumed to be approximately spherical. Furthermore it will be assumed that the density fall-off of the BHBF stars of outer stellar halo can be approximated by the power-law relation  $\rho(r) \propto r^{-\alpha}$ ,  $\alpha = 3.4 \pm 0.3$  - see SLFC94.

The potential of the outer parts of the Galaxy is assumed to be approximately spherical and logarithmic,  $\Phi(r) = V_c^2 \ln(r)$ , corresponding to a flat rotation curve of the Galaxy, with  $v_c(r) = V_c = 220 \text{ km s}^{-1}$ .

The anisotropy parameter  $\beta$  is defined as

$$\beta = 1 - \left(\frac{\sigma_t}{\sigma_r}\right)^2, \quad (1)$$

where  $\sigma_r$  is the radial and  $\sigma_t$  the (1-D) tangential velocity dispersion. Thus the Jeans equation has the form

$$\frac{1}{\rho} \frac{d(\rho \sigma_r^2)}{dr} + \frac{2\beta \sigma_r^2}{r} = -\frac{d\Phi}{dr}. \quad (2)$$

In section 2, the evidence pointed to a significant decrease in the radial velocity dispersion, from about  $140 \text{ km s}^{-1}$  at the sun to about  $90 - 110 \text{ km s}^{-1}$  in the outer halo. We use the following simple model for  $\sigma_r^2(r)$ :

$$\sigma_r^2 = \sigma_0^2 + \frac{\sigma_+^2}{\pi} \left( \frac{\pi}{2} - \tan^{-1} \left( \frac{r - r_0}{l} \right) \right). \quad (3)$$

Adopting this form gives us good flexibility in modelling the decrease in  $\sigma_r(r)$  with increasing  $r$ .

It follows from equation (3) that  $\sigma_0$  is the asymptotic value of the radial velocity dispersion for  $r \gg (r_0 + l)$  and that  $\sqrt{\sigma_+^2 + \sigma_0^2}$  approximately is the radial velocity dispersion in the inner halo ( $r \lesssim r_0$ ). The physical meaning of the two scale parameters  $r_0$  and  $l$  is given in SLFC94 and is fairly straightforward.

Substituting (3) into (2), we solve for  $\sigma_t$ :

$$2\sigma_t^2 = V_c^2 - \sigma_r^2(\alpha - 2) - \frac{1}{\pi} \frac{r}{l} \frac{\sigma_+^2}{(1 + ((r - r_0)/l)^2)}. \quad (4)$$

The line-of-sight velocity dispersion of a set of stars in a field at Galactic coordinates  $(l, b)$  where the velocity ellipsoid has components  $\sigma_r$  and  $\sigma_t$  is

$$\sigma_{\text{los}}^2 = \gamma^2 \sigma_r^2 + (1 - \gamma^2) \sigma_t^2, \quad (5)$$

where  $\gamma$  is a simple geometric projection factor given by

$$\gamma = (d - r_\odot \cos l \cos b) / r. \quad (6)$$

The mean values of  $\gamma$  for the various bins are given in Table 1.

We have fitted the above model to the much larger data sample considered in this paper using a maximum likelihood approach, assuming a radial velocity dispersion at the sun,  $r = r_\odot$ , of  $\sigma_{r,\odot} = 140 \text{ km s}^{-1}$ , as in SLFC94, and hence reducing the number of free parameters of the model to three.

The best-fit model is shown in Figure 1, where we show  $\sigma_r(r)$  as a solid line and  $\sigma_t(r)$  as a dashed line. The best-fit parameters are  $r_0 = 13.5 \text{ kpc}$ ,  $l = 7.5 \text{ kpc}$ ,  $\sigma_0 = 89 \text{ km s}^{-1}$  and  $\sigma_+ = 129 \text{ km s}^{-1}$ . The radial velocity dispersion decreases from  $148 \text{ km s}^{-1}$  in the inner halo to an asymptotic value  $89 \text{ km s}^{-1}$  at large  $r$ ,

whereas the tangential velocity dispersion increases from about  $91 \text{ km s}^{-1}$  in the inner halo to about  $137 \text{ km s}^{-1}$  in the outer halo. The radial velocity dispersion,  $\sigma_r$ , decreases fairly rapidly beyond the solar circle, with a corresponding increase in  $\sigma_t$ . The model predicts a tangential velocity dispersion at the sun,  $r = r_\odot$ , of  $\sigma_{t,\odot} = 93 \text{ km s}^{-1}$ , in good agreement with the measured value for this quantity (see section 2), which is about  $90\text{--}100 \text{ km s}^{-1}$ .

In Figure 2  $\sigma_{\text{los}}$ , as predicted by the model, is shown as the solid lines for the fields described in section 2. The circles are the data, the vertical error bars being the observational  $1\text{-}\sigma$  error in the determination of  $\sigma_{\text{los}}$  and the horizontal bars the  $1\text{-}\sigma$  error in the mean distance for the stars in the various bins. The value of  $\chi^2$  for the model is 8.0 (13 degrees of freedom), a very good fit, as can also be seen from inspection of Figure 2.

## 4 Discussion

### 4.1 The dynamics and kinematics of the outer stellar halo

The main result of the analysis is that  $\sigma_r$  decreases fairly rapidly beyond the solar circle – already by  $r \simeq 20 \text{ kpc}$  it has dropped to approximately  $110 \text{ km s}^{-1}$ ; by  $r \simeq 40 \text{ kpc}$  it has decreased to about  $90 \text{ km s}^{-1}$ . This conclusion is very firm because the radial velocities in our outer fields are dominated by  $\sigma_r$ . The tangential velocity dispersion,  $\sigma_t$ , is expected to rise correspondingly rapidly in this region in order to be consistent with a flat rotation curve. We note here that the decrease in  $\sigma_r$  and increase in  $\sigma_t$  actually takes place within  $r \lesssim 20 \text{ kpc}$ , where the rotation curve is observationally well constrained to be flat (Fich & Tremaine 1991).

We find that the  $1\text{-}\sigma$  error on  $\sigma_0$  is  $\pm 19 \text{ km s}^{-1}$ , *i.e.*,  $\sigma_r$  decreases from  $140 \pm 10 \text{ km s}^{-1}$  at the sun to about  $89 \pm 19 \text{ km s}^{-1}$  at large  $r$ . Hence, the most important kinematic feature of the model is that the velocity ellipsoid changes from *radial* anisotropy in the solar vicinity ( $\beta \simeq 0.5$ ) to *tangential* anisotropy in the outer halo ( $\beta \simeq -1.3$ ).

To illustrate this further, we have calculated the predictions of two, alternative ‘toy’ models. For these models we assumed that the velocity ellipsoid is constant with  $r$ , rather than depending quite strongly on  $r$ , as for the dynamical model presented in SLFC94 and in this paper. For the first ‘toy’ model  $\vec{\sigma} = (150, 100, 100) \text{ km s}^{-1}$  (in spherical polars) was assumed, as indicated by the findings of Beers & Sommer-Larsen (1995). The second ‘toy’ model was identical to the first, except that it had  $\sigma_r = 140 \text{ km s}^{-1}$ , since this value of  $\sigma_r$ , at  $r = r_\odot$ , was adopted in our main model, as described previously in this section.

We compared the predictions of the ‘toy’ models with the data by calculating the value of  $\chi^2$  obtained. For the first ‘toy’ model  $\chi^2 = 46.5$  (13 degrees of freedom) implying that it can be rejected at the 99.999 % confidence level. For the second  $\chi^2 = 33.8$  (13 degrees of freedom), so this model can ‘only’ be rejected

with 99.9 % confidence. Clearly, such models are not viable and this, of course, is the main reason why the dynamical model of Sommer-Larsen (1987), where  $\vec{\sigma}$  has a rather strong dependence on  $r$ , and all subsequent similar models (including the one discussed in this paper), has been proposed.

## 4.2 Outer stellar halo kinematics: clues towards understanding the formation of the Milky Way

Our results concerning the dynamics and kinematics of the outer stellar halo are of considerable interest in relation to theories of the formation of the Milky Way, in particular, and galaxies in general.

If the Galaxy formed from a single collapsing over-density region in the early universe, then one might expect the outer halo to be characterized by significantly-radially-anisotropic kinematics (see, e.g., van Albada 1982), whereas the data show that quite the opposite is the case. If, on the other hand, at least the outer parts of the proto-Galaxy were assembled by accretion of various lumps, then a large tangential velocity dispersion in the outer parts of the Galaxy is possible, depending on the nature of the accretion (Norris 1994; Freeman 1996). So our results indicate that the outer stellar halo formed by some sort of accretion and merging processes. The kinematics of stars in the inner halo are, at least locally, radially anisotropic, possibly indicating that the inner parts of the halo formed during a more dissipative and coherent collapse, probably on a relatively short (dynamical) time scale and possibly in concert with ongoing accretion and merging processes in the inner halo as well.

Chemical evolution arguments lead to a similar conclusion on the basis of the finding that there is a significant abundance gradient in the inner halo, but essentially none in the outer halo. This was discussed in the pioneering work by Searle & Zinn (1978) and in much subsequent work - see, e.g., Norris (1996) and references therein.

In the following we discuss various aspects of the formation of the Galaxy in more detail.

It is possible that the major part of the inner gas ended up in the Galactic bulge as the bulge and the local stellar halo have very similar specific angular momentum distributions (Wyse & Gilmore 1992; Ibata & Gilmore 1995).

The formation of the outer stellar halo may, on the one hand, not necessarily be related to the formation of the Galactic disk, since the thick disk apparently contains stars of very low metallicity – comparable to or perhaps lower than the average abundance of the globular clusters (Beers & Sommer-Larsen 1995). On the other hand, the globular clusters are not likely to be representative of the stellar halo (see below) and it seems somewhat more direct and reasonable to assume that the Galactic disk mainly *did* form out of gas, initially located in subsystems gradually merging in the inner part of the increasingly deep, dark-



matter potential well. In the following we shall consider this latter and, perhaps, most relevant option in more detail.

It is likely that the Galactic globular clusters survived to the present only because they are so compact, whereas the more diffuse and probably lower-metallicity subsystems, which contained the major part of the gas available for the formation of the Galactic disk (see below), broke up quite early due to effects of star-formation feedback processes, tidal destruction, dynamical friction etc. (see also Freeman 1996). The bulk of gas in these systems most likely was left in a dilute, non star-forming, state after the disruption and subsequently gradually settled as a large and massive, differentially rotating disk.

The mass of the Galactic globular cluster system is only of order 0.2 % of the mass of the Galactic disk, so the globular clusters are likely to be highly unrepresentative of the typical accreted subsystems.

Furthermore the mass of the stellar halo is of the order 2 % of the mass of disk, indicating that only a tiny fraction of the gas in the more typical subsystems was locked up as stars prior to the disruption of the subsystems.

The famous, solar neighbourhood, G-dwarf problem is most readily resolved if it is assumed that gas continued to settle onto the Galactic disk over a period, which is shorter than, but comparable to, the age of the disk (e.g. Pagel & Patchett 1975; Sommer-Larsen 1991; Rocha-Pinto & Maciel 1996). If this indeed is the correct resolution of the G-dwarf problem, then the settling of the gas from the disrupted subsystems onto the Galactic disk was quite gradual, as proposed above.

The key question seems to be: From where did the large amount of angular momentum of the Galactic disk originate ?

It follows from the work of Sommer-Larsen & Zhen (1990) that the time-averaged galactocentric distance of local halo stars is, in general, smaller than  $r_{\odot}$ . The average rotation velocity of the local halo stars is very small, perhaps even negative, (e.g. Sommer-Larsen & Christensen 1989; Beers & Sommer-Larsen 1995) and hence so is their average specific angular momentum. Consequently, the gas associated with the formation of the local halo stars, at  $r \lesssim r_{\odot}$ , most likely did not end up in the Galactic disk. Indeed, as argued above, this gas probably ended up in the bulge.

So, in this scenario, the bulk of the disk gas originated from the disrupted subsystems that formed the outer stellar halo. Consequently these systems, taken as a whole, were carrying an amount of angular momentum, probably mainly in orbital form, which was at least as large as that of the present Galactic disk. The following simplistic discussion indicates that this prediction can be tested observationally.

The surface density distribution of a truncated, exponential disk, as a function

of radial coordinate  $R$ , is given by

$$\Sigma(R) = \begin{cases} \Sigma_0 \exp(-R/R_d) , & R < R_t \\ 0 & , \quad R \geq R_t \end{cases} \quad (7)$$

where  $\Sigma_0$  is the central surface density,  $R_d$  the exponential scale length and  $R_t$  the truncation radius. The stellar component of large galactic disks is typically truncated at  $R_t \sim 4R_d$ . Since the mass of the stars in the Galactic disk is much larger than that of the gas, we neglect, for simplicity, the latter component in this discussion. Assuming a constant rotation curve, i.e.  $v_c(R) \simeq V_c = c^{st}$ , it is easy to show that the specific angular momentum of the disk is

$$j_d = \xi(q) R_d V_c \quad , \quad q = \frac{R_t}{R_d} \quad , \quad (8)$$

where  $\xi(q) = 1.44, 1.68$  and  $1.82$  for  $q = 3, 4$  and  $5$  respectively (and  $\xi(q) \rightarrow 2$  for  $q \rightarrow \infty$ ).

Let the typical galactocentric distance of disruption of the Galactic disk progenitor systems be denoted  $r_{disrupt}$ . The results obtained in this paper suggest that the kinematics of the stars of the outer halo are quite tangentially anisotropic ( $\beta \sim -1.3$ ) and hence that the average galactocentric distance of the halo stars originating from the disk progenitor systems is approximately equal to  $r_{disrupt}$ . The mean specific angular momentum of the dilute gas, originating from the disrupted subsystems and later settling onto the disk, is likely to be approximately conserved during this infall phase (contrary to the case where the gas is spiraling inwards as dense satellites, continuously losing orbital angular momentum and energy to the dark matter halo by dynamical friction - see, e.g., Navarro & White 1994). Denoting the mean rotational velocity of the halo stars at  $r \sim r_{disrupt}$  by  $\bar{v}_{rot} = \langle v_\phi \rangle$  it then follows that

$$j_d \sim r_{disrupt} \bar{v}_{rot} \quad , \quad (9)$$

so

$$\bar{v}_{rot} \sim \frac{\xi(q) R_d V_c}{r_{disrupt}} = 49 \left( \frac{\beta(q)}{1.68} \right) \left( \frac{R_d}{4 \text{ kpc}} \right) \left( \frac{V_c}{220 \text{ km/s}} \right) \left( \frac{r_{disrupt}}{30 \text{ kpc}} \right)^{-1} \text{ km/s} . \quad (10)$$

To briefly recapitulate the essentials of the observational test: If  $\bar{v}_{rot} \gtrsim 50 \text{ km s}^{-1}$  in the outer halo, then it appears quite likely that the subsystems, from where the stars in the outer halo originated, were the main progenitors of the Galactic disk. Conversely, if  $\bar{v}_{rot}$  is much smaller than this, perhaps even negative, in the outer halo (like for the local halo stars), then it seems unlikely that the progenitor subsystems of the outer stellar halo were also the main progenitors of the Galactic disk.

Unfortunately, it is doubtful that this prediction can be tested on the basis of observed line-of-sight velocities of outer halo BHBF stars, since, as discussed previously, the line-of-sight velocity is essentially the radial velocity,  $v_r$ , at large  $r$ . To determine  $\bar{v}_{rot}$  observationally, on the basis of proper motions, requires a measurement accuracy of about  $10^{-4}$  "/yr, so this is clearly not possible on the basis of photographic plates, even with a  $\sim 100$  yr baseline. Nor can it be done using the Hipparcos satellite, as the stars are quite faint ( $B \simeq V \sim 18$  mag), and as the measuring accuracy of even Hipparcos is an order of magnitude too low for this purpose. But the discussion above suggests that it would be of considerable relevance and importance to bear in mind this observational test, based on outer halo stars, when planning future proper motion measuring systems.

All in all our results may be interpreted as supporting the notion that the Galaxy formed hierarchically (partly or fully), preying on smaller subsystems - the 'bottom-up' galaxy formation scenario (see, e.g., Blumenthal et al. 1984 for an excellent review of various galaxy formation scenarios), which for quite a while has been considered the favorite by the majority of theorists working on galaxy formation and recently also has been given some observational credibility through HST observations of a potential group of small galaxies, at high redshift, possibly in the process of merging to a larger galaxy (Pascarelle et al. 1996).

## 5 Conclusion

We have analysed the kinematics and dynamics of the system of blue horizontal branch field (BHBF) stars in the outer Galactic halo using a large sample ( $\sim 700$ ) of BHBF stars.

The basic result is that the radial component,  $\sigma_r$ , of the stellar halo's velocity ellipsoid decreases fairly rapidly beyond the solar circle, from  $\sigma_r \simeq 140 \pm 10$  km s $^{-1}$ , at  $r = r_\odot$ , to an asymptotic value of  $\sigma_r = 89 \pm 19$  km s $^{-1}$  at large  $r$ . This result is very firm, because at large  $r$ ,  $\sigma_{los}$  is dominated by  $\sigma_r$ . Assuming that the rotation curve of the Galaxy is approximately flat, the fairly fast decrease in  $\sigma_r$  is matched by an increase in the tangential velocity dispersion,  $\sigma_t$  with increasing  $r$ . We conclude that the stellar halo velocity ellipsoid changes markedly, from radial anisotropy ( $\beta \simeq 0.5$ ) at the sun, to tangential anisotropy ( $\beta \simeq -1.3$ ) in the outer parts of the Galactic halo ( $r \gtrsim 20$  kpc).

The implications of our results for possible Galactic formation scenarios are discussed. Our results may indicate that the Galaxy formed hierarchically (partly or fully) through merging of smaller subsystems - the 'bottom-up' galaxy formation scenario, which for quite a while has been favoured by most theorists and recently also has been given some observational credibility by HST observations of a potential group of small galaxies, at high redshift, possibly in the process of merging to a larger galaxy (Pascarelle et al. 1996).

The results obtained in this paper are very similar to what SLFC94 found

based on a five times smaller sample of BHBF stars. It is gratifying, though, that the goodness of the model fit to the observational data has improved considerably relative to model fit in SLFC94.

The recent work of Flynn, Sommer-Larsen & Christensen (1996) strongly suggests, on the basis of numerical simulations, that such a model is physically feasible, in the sense that a stationary phase space distribution function  $f$  exists, which can generate this sort of kinematics and at the same time is non-negative everywhere in phase space. This is also strongly hinted at by the theoretical, dynamical models of Sommer-Larsen (1987) and Vedel & Sommer-Larsen (1990).

## Acknowledgements

We have benefited considerably from the comments of Bernard Pagel, Henrik Vedel, Draza Marković, Cedric Lacey and the referee. This work was supported by Dansk Grundforskningsfond through its support for an establishment of the Theoretical Astrophysics Center. T.C.B. acknowledges partial support for this work from grants AST 90-1376 and AST 92-22326 awarded by the National Science Foundation. T.C.B. would like to express gratitude for the hospitality shown by the Theoretical Astrophysics Center at the University of Copenhagen, where the work reported in this paper was conducted. R.W. acknowledges partial support from the teaching post-doctoral program at Michigan State University.

## References

- Arnold, R., & Gilmore, G. 1992, MNRAS, 257, 225
- Beers, T.C., & Sommer-Larsen, J. 1995, ApJS, 96, 175
- Beers, T.C., Preston, G.W., & Shectman, S.A. 1992, AJ, 103, 1987
- Beers, T.C., Doinidis, S.P., Wilhelm, R.J., & Mattson, C. 1996, ApJS, 103, 433
- Blumenthal, G.R., Faber, S.M., Primack, J.R., & Rees, M.J. 1984, Nature, 311, 517
- Carney, B.W., Latham, D.W., Laird, J.B., & Aguilar, L.A. 1994, AJ, 107, 2240
- Fich, M., & Tremaine, S. 1991, ARA&A, 29, 409
- Flynn, C., Sommer-Larsen, J., & Christensen, P.R. 1994, MNRAS, 267, 77
- Flynn, C., Sommer-Larsen, J., & Christensen, P.R. 1995, A&AS, 109, 171
- Flynn, C., Sommer-Larsen, J., & Christensen, P.R. 1996, MNRAS, 281, 1027
- Freeman, K.C. 1987, ARA&A, 25, 603
- Freeman, K.C. 1996, in Formation of the Galactic Halo - Inside and Out, ed. H. L. Morrison & A. Sarajedini (Astronomical Society of the Pacific: San Francisco), 3
- Hartwick, F.D.A. 1987, in The Galaxy, ed. G. Gilmore & R. Carswell (Dordrecht: Reidel), 281
- Hawkins, M.R.S. 1984, MNRAS, 206, 433
- Ibata, R., & Gilmore, G. 1995, MNRAS, 275, 605
- Kinman, T.D., Suntzeff, N.B., & Kraft, R.P. 1994, AJ, 108, 1722
- Larsen, J.A. & Humphries, R.M. 1994, ApJ, 436, L149
- Majewski, S.R., Munn, J. A., & Hawley, S. L. 1996, ApJ, 459, L73
- Morrison, H., Flynn, C., & Freeman, K.C. 1990, AJ 100, 1191
- Navarro, J.F., & White, S.D.M. 1994, MNRAS, 267, 401
- Norris, J.E. 1986, ApJS, 61, 667
- Norris, J.E. 1994, ApJ, 431, 645
- Norris, J. E. 1996, in Formation of the Galactic Halo - Inside and Out, ed. H. L. Morrison & A. Sarajedini (Astronomical Society of the Pacific: San Francisco), 14
- Norris, J., Bessell, M., & Pickles, A. 1985, ApJS, 58, 463
- Pagel, B. E. J., & Patchett, B. E. 1975, MNRAS, 172, 13

- Pascarelle, S.M., Windhorst, R.A., Keel, W.C., & Odewahn, S.C. 1996, *Nature*, 383, 45
- Ratnatunga, K., & Freeman, K.C. 1989, *ApJ*, 339, 126
- Rocha-Pinto, H. J., & Maciel, W. J. 1996, *MNRAS*, 279, 447
- Ryan, S.G., & Norris, J.E. 1991, *AJ*, 101, 1835
- Searle, L., & Zinn, R. 1978, *ApJ*, 225, 357
- Sommer-Larsen, J. 1987, *MNRAS*, 227, 21p
- Sommer-Larsen, J. 1991, *MNRAS*, 249, 368
- Sommer-Larsen, J., & Christensen, P.R. 1989, *MNRAS*, 239, 441
- Sommer-Larsen, J., Flynn, C., & Christensen, P.R. 1994, *MNRAS*, 271, 94
- Sommer-Larsen, J., & Zhen, C. 1990, *MNRAS*, 242, 10
- van Albada, T.S. 1982, *MNRAS*, 201, 939
- Vedel, H., & Sommer-Larsen, J. 1990, *ApJ*, 359, 104
- Wilhelm, R. 1995, PhD thesis, Michigan State University
- Wilhelm, R., Beers, T.C., & Gray, R. 1997, *AJ*, submitted
- Wilhelm, R., Beers, T.C., Flynn, C., Layden, A., Pier, J.R., & Sommer-Larsen, J. 1997, in preparation
- Wetterer, C.J., & McGraw, J.T. 1996, *AJ*, 112, 1046
- Wyse, R.F.G., & Gilmore, G. 1992, *AJ*, 104, 144
- Yamagata, T., & Yoshii, Y. 1992, *AJ*, 103, 117

Table 1: Line-of-sight velocity dispersions etc. for the 16 data bins

Field	$d$ [kpc]			$\langle d \rangle$ [kpc]	$\langle r \rangle$ [kpc]	$\sigma_{\text{los}}$ [km s $^{-1}$ ]	$\langle \gamma \rangle$	$N$
F117	$0 < d < 6$			$4.0 \pm 0.3$	8.9	$120 \pm 15$	0.45	39
	$6 \leq d < 12$			$8.0 \pm 0.4$	11.3	$113 \pm 10$	0.71	33
	$12 \leq d < 45$			$19.0 \pm 1.6$	20.6	$107 \pm 24$	0.92	21
22HR	$0 < d < 4$			$3.4 \pm 0.2$	7.0	$87 \pm 10$	-0.01	44
	$4 \leq d < 6$			$5.0 \pm 0.1$	7.0	$111 \pm 10$	0.15	57
	$6 \leq d < 12$			$7.8 \pm 0.2$	7.5	$116 \pm 15$	0.48	47
	$12 \leq d < 45$			$18.7 \pm 1.3$	16.3	$112 \pm 12$	0.90	29
SA287	$0 < d < 4$			$3.0 \pm 0.2$	6.3	$93 \pm 11$	-0.15	52
	$4 \leq d < 6$			$5.0 \pm 0.2$	5.9	$97 \pm 9$	-0.01	76
	$6 \leq d < 12$			$7.6 \pm 0.2$	6.2	$93 \pm 13$	0.34	66
	$12 \leq d < 45$			$16.7 \pm 0.9$	12.7	$113 \pm 20$	0.89	28
GP	$0 < d < 4$			$2.8 \pm 0.1$	8.5	$77 \pm 8$	0.33	52
	$4 \leq d < 6$			$4.8 \pm 0.1$	9.3	$95 \pm 10$	0.51	66
	$6 \leq d < 12$			$7.4 \pm 0.2$	10.9	$117 \pm 12$	0.68	43
	$12 \leq d < 45$			$17.6 \pm 2.7$	19.3	$99 \pm 19$	0.91	21
Very distant	$d \geq 45$			$55.2 \pm 2.4$	53.9	$100 \pm 23$	0.99	9

**Figure 1** Best-fit model. The solid line shows the radial velocity dispersion  $\sigma_r(r)$  and the dashed line shows the tangential velocity dispersion  $\sigma_t(r)$ .

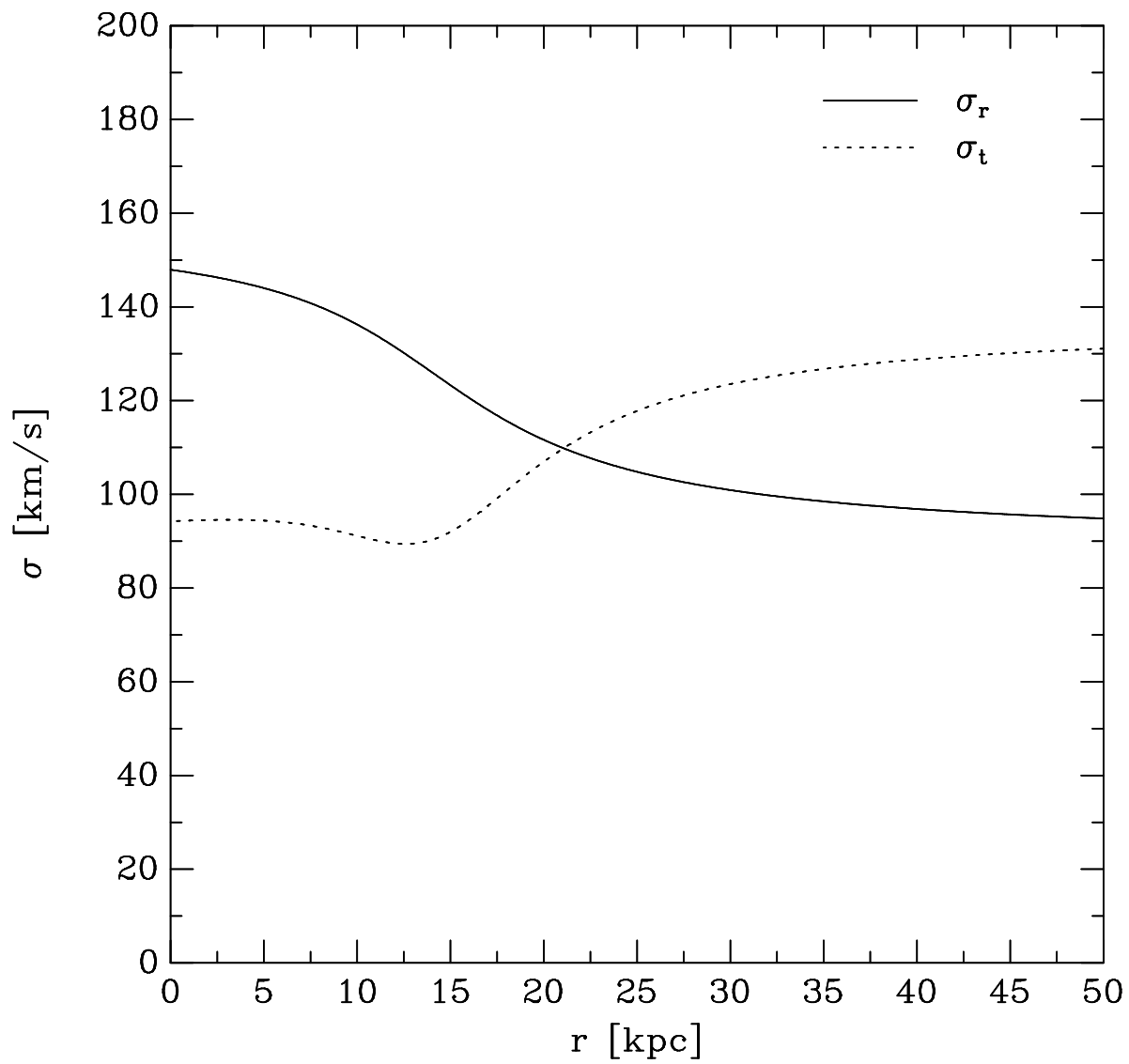




**Figure 2** The line-of-sight velocity dispersion for the best fitting model as a function of distance  $d$  along the four lines of sight (including reflections) is shown as solid lines. Solid circles show the measured values from Table 1. The vertical error bars are the  $1\text{-}\sigma$  errors in the line-of-sight velocity dispersion measurement, and the horizontal error bars are the  $1\text{-}\sigma$  errors in the mean distance of the stars in each bin. The predictions of 'toy' model #1, with  $\vec{\sigma} = (150, 100, 100) \text{ km s}^{-1}$  in spherical polars, is shown by the dotted lines. Similarly, 'toy' model #2, with  $\vec{\sigma} = (140, 100, 100) \text{ km s}^{-1}$  in spherical polars, is shown by the dashed lines.

